DEUTSCHES ELEKTRONEN-SYNCHROTRON DESY

DESY 78/65
November 1978

ON THE NUCLEON PROPAGATOR IN MESON THEORY

by

F. Gutbrod

NOTKESTRASSE 85 · 2 HAMBURG 52

To be sure that your preprints are promptly included in the
HIGH ENERGY PHYSICS INDEX ,
send them to the following address (if possible by air mail) :

DESY
Bibliothek
Notkestrasse 85
2 Hamburg 52
Germany

On the Nucleon Propagator in Meson Theory

by

F. Gutbrod

Deutsches Elektronen-Synchrotron DESY

Abstract

We solve the Bethe-Salpeter equation for the electromagnetic nucleon vertex at zero momentum transfer and determine the nucleon propagator selfconsistently. Higher order meson exchanges, which are required by the Ward identity, are taken into account.

I. Introduction

We take the point of view that the low energy or low momentum transfer properties of hadrons like electromagnetic radii, magnetic moments of baryons etc. are calculable from simple Feynman diagrams involving known particles, i.e. primarily from meson and baryon loops. For this program the knowledge of the meson and baryon propagators is obviously very important. To derive these propagators in meson theory from a perturbation expansion in $g^2/4\pi = 14.6$ is probably hopeless. It may work better to use first of all a skeleton expansion with a dressed meson-baryon vertex and with dressed propagators, the latter being secondly subject to one of the field theoretic integral equations. We expect such an expansion to converge better than perturbation theory, because due to the decrease of the dressed vertices the effective coupling constant at small distances may be considerably smaller than the on-shell coupling constant. This depends of course on the final result for the propagator. As the integral equation we choose the Bethe-Salpeter equation (BSE) for the electromagnetic vertex at zero momentum transfer, connected to the propagator via the Ward identity (WI).

For the meson propagator this procedure is fairly simple and has been treated in refs. [1] and [2]. The results obtained there depended, among many other approximations, on assumptions on the nucleon propagator, but we expect them to change only slightly if we replace our assumptions by the outcome of this paper. For the fermion vertex however there are serious spin complications. There is an identity between two of the three invariant form factors which is violated if we take for the BS-kernel the lowest order terms which are shown in fig. 1a) and 1b). (In addition to nucleon exchange 1b) also $\Delta(1236)$

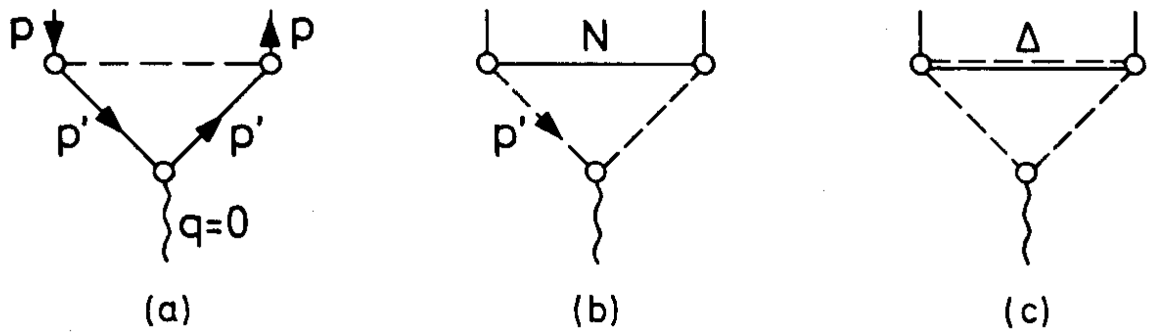

Fig. 1

Vertex diagrams with lowest order BS-kernels

exchange will be taken into account, fig. 1c)). In other words, the simple diagrams with dressed vertices violate charge conservation, and the dressed ladder BSE is not a consistent approximation. In order to restore the WI we shall consider a specific model for these vertices which leads to the inclusion of crossed meson diagrams for the BS-kernel. Our inability to calculate these diagrams exactly gives us the freedom to adjust some parameters such that current conservation is fulfilled. We then obtain a complicated set of integral equations and differential relations which we solve by iterative methods [1,3], restricting ourselves to the region $p^2 \leqslant M^2$. From the beginning we make the assumption that the propagators have anomalous dimensions, i.e. the renormalization constant Z_1 is taken as zero and the pointlike diagram is absent in fig. 1. With our subsequent choice of the strong vertex function the loops in fig. 1 are finite without subtractions, although the theory is not superrenormalizable. The charge normalization condition on mass shell is therefore a consistency check for the BS-kernel.

The two scalar functions $\tau_1(p^2)$ and $\tau_2(p^2)$ in the propagator,

$$S(p) = \not{p}\,\tau_1(p^2) + M\,\tau_2(p^2) \tag{1.1}$$

(M = nucleon mass) will behave quite differently in our model. Whereas $\tau_1(p^2)$ decreases slowly for $p^2 \to -\infty$ (it has a positive spectral function [4]), the function $\tau_2(p^2)$ drops much faster, such that the mass term in (1.1) becomes small for $p^2 \sim -10\ \text{GeV}^2$ (it has no stringent bound). This has already been found in the perturbative approach [5].
In the next section we establish the notation and discuss the simple model of fig. 1 with its shortcomings. In section 3 the crossed meson diagrams are estimated, and in section 4 the solution techniques and the results for S(p) are presented. Conclusions and an outlook for applications are given in Section 5.

II. The One Loop Model

In this section we shall collect the basic formulas for the vertex and the propagator, and the BS-kernels from fig. 1 will be evaluated. The e.m. vertex of the proton at q = 0 (see fig. 1 for definition of momenta) has three invariant form factors, and we write it as

$$\Gamma_\mu(p) = \gamma_\mu A(p^2) + 2\not{p}\,p_\mu B(p^2) - 2p_\mu M\,C(p^2)\,. \tag{2.1}$$

At $\not{p} = M$ the charge normalization condition is

$$A(M^2) + 2M^2(B(M^2) - C(M^2)) = 1 . \tag{2.2}$$

For the nucleon propagator we use two different forms,

$$\begin{aligned} S(p) &= (\not{p}\, R_1(p^2) - M R_2(p^2))^{-1} \\ &= \not{p}\, r_1(p^2) + M r_2(p^2). \end{aligned} \tag{2.3}$$

The spectral functions $\rho_i(m^2)$ for the $r_i(p^2)$ have to satisfy the positivity constraints [(4)]

$$\rho_1(m^2) \geq 0 , \tag{2.4}$$

$$\frac{m}{M}\rho_1(m^2) - \rho_2(m^2) \geq 0 . \tag{2.5}$$

The Ward identity $$\Gamma_\mu(p) = \partial_{p_\mu} S^{-1}(p) \tag{2.6}$$

gives three relations: $$R_1(p^2) = A(p^2) , \tag{2.7}$$

$$R_2'(p^2) = C(p^2) , \tag{2.8}$$

$$B(p^2) = A'(p^2) . \tag{2.9}$$

Finally $$R_1(M^2) = R_2(M^2) \tag{2.10}$$

together with (2.2) ensures the correct singularity of the propagator at $p^2 = M^2$.

In standard perturbation theory, the constraint (2.9) is valid order for order, but not necessarily so in the skeleton expansion.

In order to define this expansion we postulate that the dressed πN vertex is a pure pseudoscalar one with the following parametrization (p_1 and p_2 are nucleon momenta, m_π = pion mass)

$$\Gamma_5(p_1,p_2) = \gamma_5 V(p_1,p_2),$$
$$V(p_1,p_2) = 1/\left(1-(p_1^2+p_2^2+(p_1-p_2)^2-2M^2-m_\pi^2)/\Lambda^2\right). \tag{2.11}$$

This vertex has the reasonable property valid in perturbation theory that its variation with one squared momentum p_i^2 is negligible if one or two others are much larger than p_i^2. The singularity structure for timelike p_i^2 is not correct, but this should not concern us here too much as we are interested in the spacelike region. The parameter Λ^2 has been determined [2] by the condition that in a $\pi\pi$-$N\bar{N}$ BS-model one finds a ρ-resonance with the correct mass, and we take $\Lambda^2 = 2.1\,M^2$ from GW. Since we do not intend to work with a superrenormalizable model, the asymptotic behaviour of the meson and nucleon propagator has to be chosen such that e.g. vertex diagrams with a pointlike photon vertex are still logarithmically divergent. Here we hold the prejudice that in the BS-kernel one particle exchange diagrams are dominant at large momenta. Taking the supposed power behaviour of the meson and nucleon propagators as equal, we require

$$R_1(p^2) \sim (p^2)^{-2/3} \tag{2.12}$$

or $$r_1(p^2) \sim (p^2)^{-1/3}. \tag{2.13}$$

Consequently we repeat the ansatz made already for the meson propagator in GW,

$$\tau_1(p^2) = \frac{1}{p^2-M^2} + D_1 \ln^{1/3} \frac{p^2-M^2-10\,M_1^2}{p^2-M^2-M_1^2} + \sum_{i=2,3} \frac{D_i}{p^2-M^2-M_i^2}. \tag{2.14}$$

The parameters D_i and M_i^2 will be determined iteratively by the Ward identity, whereby the meson propagator $\Delta(p^2)$ will be kept as in GW. Furthermore we shall use a simple parametrization for the ratio $\tau_2(p^2)$ / $\tau_1(p^2)$ with 2 poles in p^2. We now can proceed to the calculation of the diagrams of fig. 1.

a) Pion exchange diagram (fig. 1a)

We only consider the proton in the loop, i.e. we take the neutron as neutral also off-shell. Then the product of the vertex and the two nucleon propagators again follows from (2.6) as

$$\begin{aligned} S(p')\,\Gamma_\mu\, S(p') &= -\partial_{p'_\mu} S(p') \\ &= -\gamma_\mu \tau_1(p'^2) - 2\not{p}'\,p'_\mu\,\tau_1'(p'^2) - 2M\,p'_\mu\,\tau_2'(p'^2). \end{aligned} \tag{2.15}$$

The loop amplitude is easily separated into A, B and C by taking traces with γ^μ, $\not{p}\,p^\mu$ and p^μ. One finds

$$A_\pi(p^2) = J_\pi \left\{ \tau_1 + \tfrac{2}{3}(1-x^2)\,p'^2\,\tau_1' \right\}, \tag{2.16}$$

$$\mathcal{B}_\pi(p^2) = \frac{1}{3p^2} \mathcal{J}_\pi \{ 4(x^2-1)\, p'^2\, \tau_1' \} , \tag{2.17}$$

$$C_\pi(p^2) = \frac{1}{p^2} \mathcal{J}_\pi \{ p \cdot p'\, \tau_2' \} . \tag{2.18}$$

Here we have defined the integral $\mathcal{J}_\pi\{\ \}$ by (see 2.11)

$$\mathcal{J}_\pi\{f\} = \frac{g^2}{4\pi} \int \frac{d^4p'}{i4\pi^3} V^2(p,p') \Delta((p-p')^2) f(p') , \tag{2.19}$$

and
$$x^2 = (p \cdot p')^2 / p^2 p'^2 . \tag{2.20}$$

In the following both the differentiations and the integrations (which are actually only twodimensional) in (2.16) to (2.18) were performed numerically with the ansatz (2.14).

b) Nucleon exchange diagram (fig. 1b)

With the same techniques we obtain

$$A_N(p^2) = \frac{2}{3} \mathcal{J}_N \{ p'^2 (x^2-1) \} , \tag{2.21}$$

$$\mathcal{B}_N(p^2) = \frac{1}{p^2} \mathcal{J}_N \{ p \cdot p' - \frac{p'^2}{3}(4x^2-1) \} , \tag{2.22}$$

$$C_N(p^2) = \frac{1}{p^2} \mathcal{J}_N \{ p \cdot p'\, \tau_2 / \tau_1 \} \tag{2.23}$$

with

$$J_N\{f\} = 2\,\frac{g^2}{4\pi}\int\frac{d^4p'}{i\,4\pi^3}\,V^2(p,\,p-p')\,\Delta'(p'^2)\,r_1((p-p')^2)\,f(p') \tag{2.24}$$

c) Δ (1236) exchange diagram (fig. 1c)

Clearly it is hard to define Δ -exchange precisely. There is no doubt that a Δ can be created by a summation of nucleon exchange diagrams in πN scattering [6], and therefore we should understand the exchange as an approximation for diagrams like fig. 2. For this πN off-shell forward scattering amplitude a dispersion relation in $(p-p')^2$ holds for fixed p^2 and p'^2 and this gives the following contributions to A, B and C:

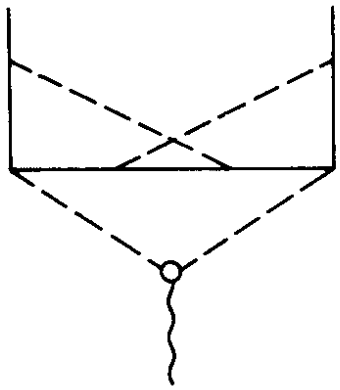

Fig. 2

Diagram leading to Δ-exchange

$$A_\Delta(p^2) = -\tfrac{2}{3}J_\Delta\{p'^2(x^2-1)\} \tag{2.25}$$

$$B_\Delta(p^2) = -\frac{1}{p^2}J_\Delta\{p.p' - \frac{p'^2}{3}(x^2-1)\} \tag{2.26}$$

$$C_\Delta(p^2) = \frac{M_\Delta}{p^2 M}J_\Delta\{p\cdot p'\} \tag{2.27}$$

with

$$J_\Delta\{f\} = \frac{4}{9}\,\frac{g^{*2}}{4\pi}\,\frac{1}{m_\pi^2}\int\frac{d^4p'}{i\,4\pi^2}\,V^2(p,p-p')\,\Delta'(p'^2)\,r_1((p-p')^2+M^2-M_\Delta^2) \tag{2.28}$$

$$\times\left[(M_\Delta^2+p'^2-p^2)^2/4M_\Delta^2 - p'^2\right]V_\Delta^2(p^2,p'^2)$$

Here M_Δ is the Δ-mass and $V_\Delta(p^2,p'^2)$ is a $\pi N\Delta$ vertex function which is taken from a BS-study [6] of πN-scattering,

$$V_\Delta(p^2, p'^2) = 1/(1-(p^2-M^2+p'^2-m_\pi^2)/4M^2) \tag{2.29}$$

We have multiplied in (2.28) this vertex with the general πN-vertex and with the dressed propagator $\tau_1((p-p')^2+M^2-M_\Delta^2)$, which is somewhat arbitrary and deserves further study. The $\pi N\Delta$ coupling constant g^* was taken from ref. [7] as $g^{*2}/4\pi = 0.26$.

We now discuss qualitatively the properties of the individual terms. We realize that with the first guess $\tau_1(p^2) = \tau_2(p^2)$ we obtain $B_N(p^2) < C_N(p^2)$. In pure perturbation theory this comes from the fact that the second term in (2.22) has the opposite sign as compared to the first one as follows from symmetric integration. Similarly one finds that B_π is smaller than C_π, and both properties persist in numerical calculations in the skeleton theory. The Δ -exchange enhances this situation further since B_Δ has the opposite sign of B_π and B_N. All this implies via (2.7) - (2.9) that in the spacelike region one has $R_2(p^2) < R_1(p^2)$. We shall discuss some consequences of this small mass term in sec. 5.
Before we could consider to solve our complicated system of equations, we have to ask whether in our model the identity (2.9), B = A' is valid. With any kind of reasonable nucleon propagator this turns out to be not the case. Instead we find

$$\sum_{\pi, N, \Delta} B(M^2) \approx \frac{1}{2} \sum_{\pi, N, \Delta} A'(M^2) \tag{2.30}$$

The origin of this discrepancy is clear: In our skeleton expansion the vertices depend also on the external momentum p, and this fact increases the derivative of A, without leading to larger values of $B(p^2)$. Because of the good convergence of the B-integrals this cannot be changed by varying the large p^2-behaviour of the propagators. Consequently we must change the BS-kernel. Let us consider a specific contribution to the πN vertex Γ_5, namely a πN loop. This leads to the diagram of fig. 3a). In order to conserve the e.m. current, we have to

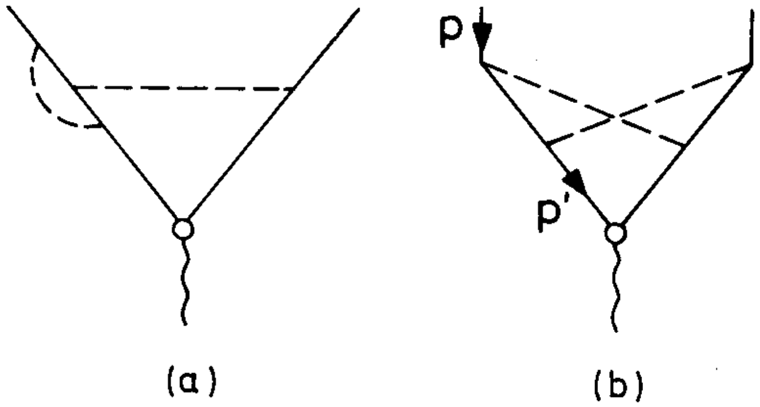

Fig. 3

Origin of crossed
meson exchange

couple the photon also to the nucleon line in the vertex, which leads to the crossed meson exchange of fig. 3b). We cannot calculate this diagram exactly nor would that be too helpful, since it certainly is not the only important addendum. In the next section we analyse its spinor structure, parametrize it conveniently and determine the parameters such that (2.9) is fulfilled. This parametrization we deduce from a rough calculation.

III. The Crossed Meson Exchange

The diagram of fig. 3b) leads to a rich spinor structure of the BS-kernel. The Feynman amplitude is

$$\frac{g^4}{i(2\pi)^4}\int d^4q\,\left(\frac{\not{p}+\not{p}'}{2}-\not{q}-M\right)\phi_\mu(p')\left(\frac{\not{p}+\not{p}'}{2}+\not{q}-M\right)F(p,p',q), \tag{3.1}$$

where q is the relative momentum of the two exchanged mesons, and

$$\phi_\mu(p') = S(p')\,\Gamma_\mu(p')\,S(p'). \tag{3.2}$$

The scalar function F(p,p',q) contains the scalar parts of the propagators and is even in q. In order to evaluate (3.1) we neglect terms like $(p\cdot q)^2$ in F(p,p',q) which is a reasonable approximation for not too large p, p' because of the large nucleon mass. This allows symmetric integration over q and leaves us with four different terms. We list then according to their Dirac decomposition (omitting ϕ_μ) with the abbreviation

$$-\frac{g^2}{i(2\pi)^4}\int d^4q\,F(p,p',q) \equiv \int_F . \tag{3.3}$$

i) The scalar part

$$S(p,p') = -\lambda_s\,M^2\,\mathbb{1}\otimes\mathbb{1}\int_F . \tag{3.4}$$

It behaves like a scalar meson exchange and is attractive. λ_s is an ad hoc normalization constant which will be discussed below.

ii) The vector part

$$V(p,p') = \frac{\lambda_V}{4}\, \gamma^{\nu} \otimes \gamma_{\nu} \int_F q^2 . \tag{3.5}$$

This acts like a vector meson exchange with a wrong sign (repulsive), which is due to the opposite flow of q in the two nucleon propagators.

iii) The scalar derivative part

$$D(p,p') = -\frac{\lambda_D}{4} (\not p + \not p') \otimes (\not p + \not p') \int_F . \tag{3.6}$$

iv) The mixed part

$$M_i(p,p') = \frac{\lambda_M}{2} M \left((\not p + \not p') \otimes \mathbb{1} + \mathbb{1} \otimes (\not p + \not p') \right) \int_F . \tag{3.7}$$

These four spinor structures add quite differently to the A, B and C amplitudes, as we shall indicate qualitatively (the full formulae are in the Appendix). We note that the superconvergent integral $\int_F$ drops rapidly with p'^2, therefore the scalar part S increases A and A' somewhat, and, because of missing γ_5 as compared to π -exchange, gives a negative result for C. This amplitude is further reduced by the vector term, which also has a large negative A content (due to the factor q^2 in the integral it does not converge quickly). The derivative term D is very important since $\not p \gamma_\mu \not p = 2 \not p p_\mu - p^2 \gamma_\mu$, where the first part directly enters the B amplitude positively, and the second part lowers A and especially A'. Thus D essentially restores (2.9). The $\not p'$ terms have a large positive A-content of short range, which we expect to be cancelled roughly by the vector part V since both terms come from the two intermediate nucleon momenta in fig. 3b which can be taken as independent integration variables instead of q and p'. Therefore they do not survive symmetric integration. Finally the mixed term M_i mainly adds to C because of $\{\not{P}\gamma_\mu\}_+ = 2P_\mu$.

In principle the individual weights λ_S to λ_M should all be 1 , and $\int_F$ and $\int_F q^2$ should be calculated numerically. Instead of this we have calculated $\int_F$ and $\int_F q^2$ for some special values of p^2 and p'^2 by keeping only the S-wave in the $\pi\pi$ channel. Relative to this reference amplitude λ_D must be roughly 2 in order to satisfy (2.9). This is not alarming, but one may speculate whether higher order corrections might change the crossed box. First of all one verifies easily that a term $(\not{P}'-M)\gamma_5(\not{P}-M)$ in the πN vertex with the sign given by the lowest order vertex loop will increase the S, D and M_i parts. (Such a term will have little effect in the nucleon box for the $\pi\pi$ channel[(2)], as it does not contribute to the leading N$\bar{\text{N}}$ s-wave state). On the other hand the diagrams of fig. 4 give rise to large cancellations in those terms of (3.1) which are proportional to M or M^2. This will be shown in the Appendix. A derivative term in the πN vertex will of course also enter into the basic triangle diagrams fig. 1a and 1b, but we shall omit these terms until a thorough discussion of the πN vertex is completed. We therefore proceed in the following way: λ_S will be taken as 1, but S will be multiplied by a strongly decreasing function of p^2 and p'^2. The ratio of λ_V and λ_D is choosen such that the A-contributions at large p'^2 cancel, whereas λ_D is ad-

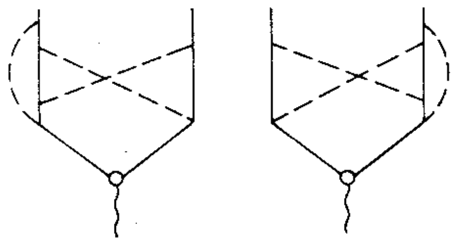

Fig. 4

Corrections to crossed meson exchange

justed via (2.9). λ_M is choosen close to 1 being "fine tuned" by the charge normalization condition (2.2). Thus λ_D and λ_M have to be readjusted slightly when we iterate our system or equations. The final set of parameters will be shown in the next section. We only remark here that finally the contribution of the crossed box are of the order of - 10 % in A and, for $p^2 > 0$, + 20 % in B and C. Only at $p^2 \ll -M^2$ the box terms become more important in B and C, where the pion and nucleon diagrams decrease quickly. Thus the fourth order contribution is, even after multiplication by 2, really a correction.

IV. Results for the Vertex and the Propagator

In compact form our problem is to solve

$$(A(p^2), B(p^2), C(p^2)) = \sum_{i=1}^{2} \int_{p'} K_i^{(A,B,C)}(p,p')\, r_i(p'^2) \tag{4.1}$$

together with the relations (2.3) to (2.9). The kernels $K_i^{(A,B,C)}(p,p')$ are given in (2.16) to (2.28) and in the Appendix. An iterative solution of this system is the only promising way. The situation is quite favourable since the equations behave stable under variations: Imagine we have found two functions $r_1(p^2)$ and $r_2(p^2)$ which solve (2.3) to (2.9) and (4.1). If we change $r_1(p^2)$ by a high mass pole, say

$$r_1(p^2) \rightarrow r_1(p^2) + \delta/(p^2 - \lambda M^2) \tag{4.2}$$

with $\delta > 0\,, \quad \lambda \gg 1\,,$

then $A(p^2)$ will decrease less steeply with p^2, and correspondingly the output propagator $r_1(p^2) \underset{p^2\to\infty}{\sim} 1/p^2 A(p^2)$ becomes closer to the free one, which would correspond to an output $\delta < 0$. Similar arguments hold for the ratio $r_2(p^2)/\ r_1(p^2)$ as can be seen from (2.23). The mathematical framework for this iterative procedure has recently been given by Stichel [12].

In order to calculate the propagator functions $r_1(p^2)$ and $r_2(p^2)$ via (2.8), the above ratio was parametrized in the form

$$r_2(p^2)/r_1(p^2) = 1 - (p^2 - M^2)\{\delta_1/(p^2-\mu_1^2) + \delta_2/(p^2-\mu_2^2)\} \tag{4.3}$$

and with a trial choice for the parameters therein and in (2.14) the form factors $A(p^2)$ to $C(p^2)$ were calculated. Then the difference $C(p^2) - B(p^2)$ was interpolated numerically by 4 pole terms and then $R_2(p^2)$ was calculated from

$$R_2(p^2) = R_1(M^2) + \int_{M^2}^{p^2} dx\,(C(x) - B(x))_{Interp.} \,. \tag{4.4}$$

In this way small violations of (2.9) drop out, since under a change of parameters $B(p^2)$ and $C(p^2)$ change essentially in parallel. $R_1(p^2)$ is simply given by (2.7). Thus the output values of $r_1(p^2)$ and $r_2(p^2)$ were determined by (2.3) and the averages between them and the trial values was used as a new input. After one or two iterations the normalization constants λ_D and λ_M ((3.6) and (3.7)) were readjusted to satisfy (2.2) and (2.9). This procedure converges very well. In figs. 5 and 6 we give the resulting propagator functions $r_1(p^2)$ and $r_2(p^2)/\ r_1(p^2)$ together with the difference between input and output functions. The coefficients of the parametrization (2.14) for

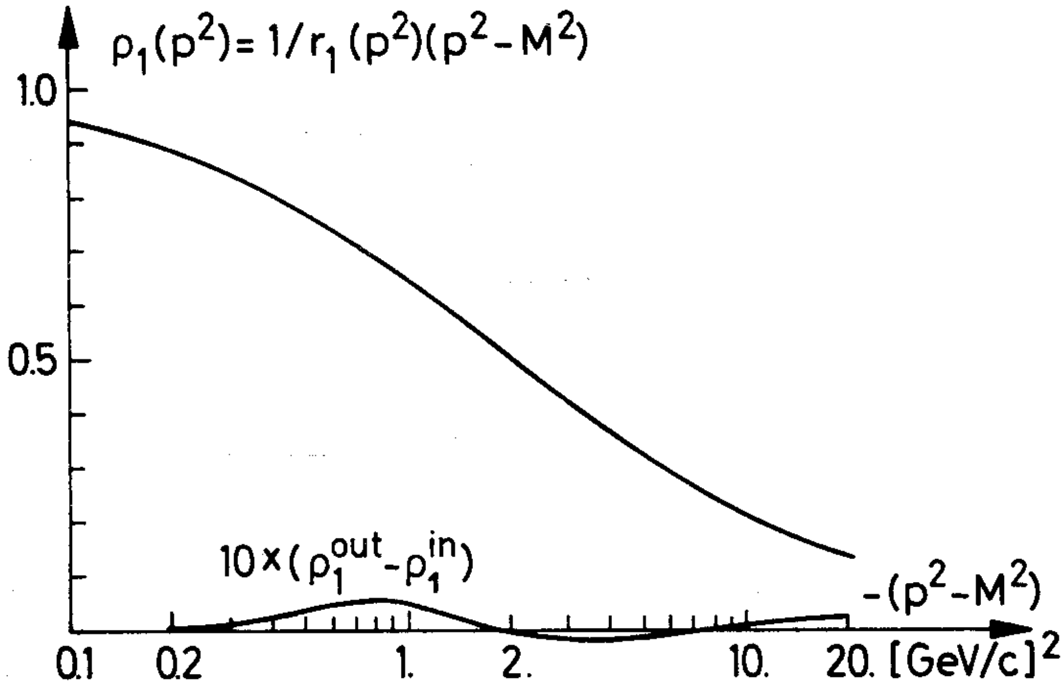

Fig. 5

Ratio of free propagator to dressed one, $\not p$-term

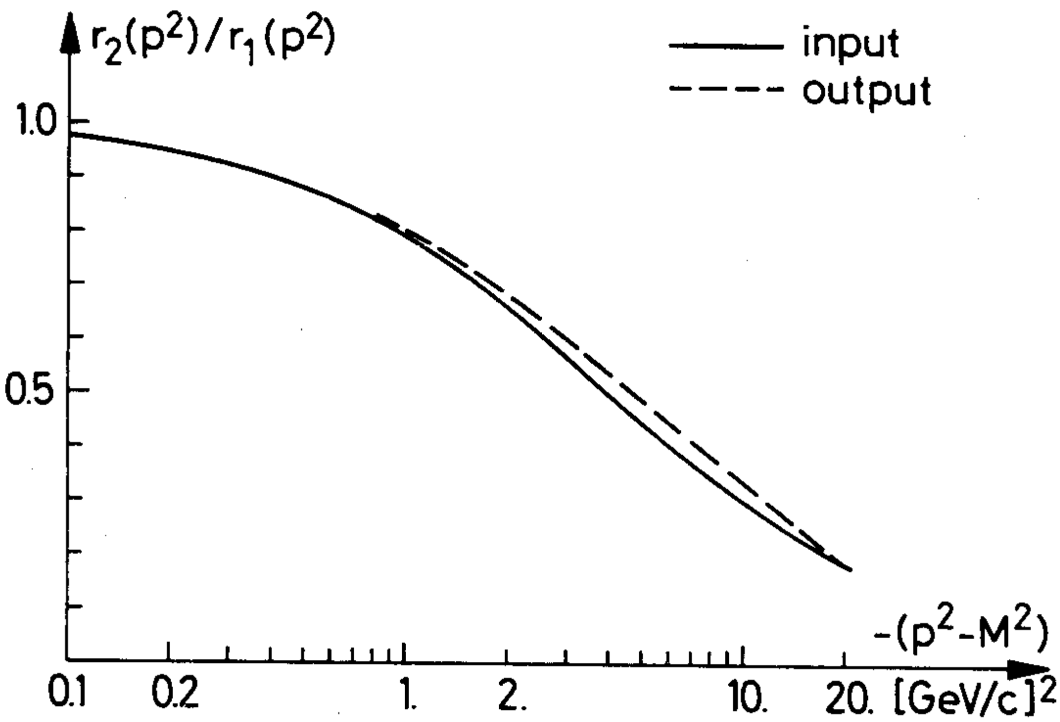

Fig. 6

Ratio of mass term to $\not p$-term

the propagator are collected in Table I as well as the constants δ_i and μ_i. For comparison we also list the parameters for the pion propagator [2]. The pion propagator after the proper mass shift, is closer to the free one

	Meson		Nucleon			
	$\Delta(p^2)$		$\tau_1(p^2)$		$\tau_2(p^2/\tau_1(p^2)$	
i	D_i	M_i [GeV]	D_i	M_i [GeV]	δ_i	μ_i [GeV]
1	0.0045	1.71	0.0057	1.71	0.9	2.1
2	0.1	0.98	0.32	1.1	0.1	4.5
3	4.0	8.8	4.3	10.8	-	-

Table I. Parameters for the meson and nucleon propagators. See eq. (2.14) for $\Delta(p^2)$ and $\tau_1(p^2)$, and (4.3) for $\tau_2(p^2)/\tau_1(p^2)$.

as the nucleon propagator, especially for small p^2. This is connected with the absence of the low mass πN continuum in the pion spectral function. The mass term $\tau_2(p^2)$ becomes uncertain at high p^2 since we only can calculate the derivative $R_2'(p^2)$, and consequently large numbers are to be subtracted for $p^2 \rightarrow -\infty$. This explains the large difference between the input and the output values for $\tau_2(p^2)/\tau_1(p^2)$ as shown in fig. 6. It may be interesting to compare the form factor $A(p^2)$ with the strong vertex function $V(P,P)$ in (2.11), which are presumably similar since for both the one pion exchange diagram is attractive and even the crossed box diagrams have the same sign. It is satisfying to see in fig. 7 that with

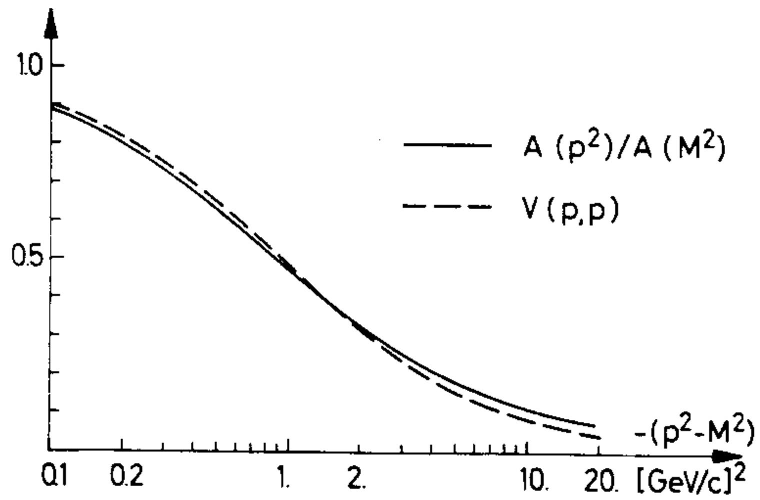

Fig.7

Comparison of e.m. and γ_5-vertex function

$\Lambda^2 = 2.1\ M^2$ the two vertex functions have indeed essentially the same p^2 dependence up to $p^2 \approx -3\ M^2$. For larger p^2 the different asymptotic behaviour of V(p,p) and $A(p^2)$ of course becomes apparent. If we nevertheless take $A(p^2)$ representative for the strong vertex we can study the consistency of our theory. For instance if we reduce Λ^2 to $\Lambda^2 = M^2$, say, and determine a new propagator, then the new $A(p^2)$ will decrease much more slowly than the new V(p,p). Thus the value of $\Lambda^2 = 2.1\ M^2$, as presently determined from the ρ-dynamics may actually come out from a selfconsistent solution of the $\pi N\bar{N}$ vertex BSE.

V. Discussion

We have shown that a BS-kernel for the coupled $\pi\pi$ and $N\bar{N}$-system can be found which allows a selfconsistent solution for the e.m. vertex BSE obeying the WI. The dominant part of the interaction is still given by one meson or one nucleon exchange, and the necessary additional spinor structures are qualitatively in accord with the crossed meson exchange diagram. Their most important effect lies in the derivative couplings of the interaction. The "cut-off" parameter Λ^2 which determines the effective $\pi N\bar{N}$ vertex at large momenta and thus partly governs the strength of the interaction, is taken from a dynamical model for the ρ-meson. The resulting nucleon propagator in the spacelike region is characterized by an increase by a factor of 2 compared to the free one at $p^2 \approx -M^2$ for the γ_4-term (see fig. 5) and by a decrease of the mass term relative to the γ_4-term by a factor 1/2 at $p^2 \approx -3\,M^2$.

In the past only rather restricted sets of diagrams have been considered (8-11), mostly nested bubble diagrams for the propagator. This would correspond in our formulation to the BSE-ladder approximation with a bare meson propagator and bare vertices, leading to divergent vertex integrals. The difficulties of such an unsymmetric expansion - only propagator corrections, but no vertex corrections - show up in the occurrence of ghosts in refs. (8-11). Such ghosts, i.e. propagator poles on the physical sheet different from the nucleon pole, could here only come from zeros of the functions R_1 and R_2. In ordinary perturbation theory with on-shell subtractions these zeros arise easily by a cancellation of the bare vertex term and subtracted vertex corrections, which become large and negative in the spacelike region. Since we set $Z_1 = 0$ from the beginning, i.e. subtract the vertex at infinite momenta and omit the bare term, zeros in the vertex could only come from a repulsive part in the BS-kernel which is not present in low orders. We have to pay for this by difficulties in the charge normalization condition, which restricts the kernel. Stated differently we assume that the hadronic vertex functions cancel the divergences that would arise from dressing only the propagators and conspire with crossed exchange diagrams etc. to conserve the charge.

Possible applications of our results to low energy hadron physics will only be mentioned shortly here, some will be published soon. We can now try, with confidence, to calculate the contribution of the pion e.m. current to the nucleon isovector form factors (magnetic moments, radii etc.). For this especially the mass term $R_2(p^2)$ is important, as it leads to non-pole terms in the π N-amplitudes which strongly affect the Pauli form factor $F_2(q^2)$. Another challenge is a direct calculation of the pion weak decay constant f_π by fermion loops, which again crucially relies on the mass term. Finally the deeply bound state problem for the $N\bar{N}$ system (i.e. the vector mesons) can be attacked, beyond that what we have done already for the ρ- meson.

The question whether our basic assumptions, i.e. pseudoscalar πN-Lagrangian, usefulness of the skeleton expansion, simple form of the dressed πN-vertex, are realistic will not be discussed here. But inside that framework there are many possibilities for improvement. One crucial problem is the e.m. structure of the neutron or the isospin structure of the BS-kernel. For the crossed diagram with modifications this is rather subtle, but it seems that in total the isoscalar charge is too large. The crossed box gives a negative contribution to the proton charge in contrast to naive expectation and the likely explanation is that the vector term (3.5) is overestimated. Lowering it would give an attractive "potential" in the isovector $N\bar{N}$-channel and Λ^2 would have to be lowered. Furthermore the $N\bar{N}$ annihilation in the isovector state is presently given only by the dressed $\pi\pi$-channel. The inclusion of more states also would lower Λ^2 and reduce the isoscalar charge if we could prove in our model that the annihilation in the $I = 0$ channel were smaller than for $I = 1$. Finally a better understanding of the πN-vertex in a BSE-model can certainly be achieved, especially with respect to induced derivative couplings.

Appendix

Here we give more details how we estimate the various spin terms in the decomposition of the crossed box diagram. First of all the break-up of the four terms S to M_i into the amplitudes A, B and C will be given in Table II. If the four $N\bar{N}$-interactions are written in the form

$$S = -\mathbb{1} \otimes \mathbb{1}\, M^2 F_S\,(P, P') \tag{A1}$$

$$V = \frac{1}{4} \gamma^\nu \otimes \gamma_\nu\, F_V\,(P, P') \tag{A2}$$

$$D = -\frac{1}{4} (\not{P} + \not{P}') \otimes (\not{P} + \not{P}')\, F_D\,(P, P') \tag{A3}$$

$$M_i = \frac{1}{2M} \left\{ (\not{P} + \not{P}') \otimes \mathbb{1} + \mathbb{1} \otimes (\not{P} + \not{P}') \right\} F_\mu (P, P') \tag{A4}$$

then the following table gives the integrands for A, B and C, after using (2.15) (again $x^2 = (P \cdot P')^2 / P^2 P'^2$):

Table II

	A	B	C
S	$(\tau_1 + X_1 P'^2 \tau_1') F_S$	$\frac{P'^2}{P^2} X_2 \tau_1' F_S$	$-\frac{1}{P^2} P \cdot P' \tau_2' F_S$
V	$\frac{1}{2}(\tau_1 + X_1 P'^2 \tau_1') F_V$	$\frac{P'^2}{2P^2} X_2 \tau_1' F_V$	$\frac{1}{P^2} P \cdot P' \tau_2' F_V$
D	$-\frac{1}{4}\{((P+P')^2 - X_1 P'^2)\tau_1 + (P^2 - P'^2) X_1 P'^2 \tau_1'\} F_D$	$\frac{1}{4P^2}\{((P+P')^2 - 2P'^2 X_1)\tau_1 - ((P^2+2P'^2)X_1 - (P+P')^2) P^2 \tau_1'\} F_D$	$-\frac{1}{4}(P+P')^2 \frac{P \cdot P'}{P^2} \tau_2 F_D$
M_i	$-X_1 P'^2 \tau_2' F_M$	$-\frac{1}{P^2}(X_2 P'^2 + P \cdot P') \tau_2' F_M$	$\frac{1}{2P^2 M^2}\{(P^2 + P \cdot P')\tau_1 + 2P \cdot P'(P \cdot P' + P'^2)\tau_1'\} F_M$

$$X_1 = \frac{2}{3}(1 - x^2)$$
$$X_2 = \frac{1}{3}(4x^2 - 1)$$

In order to get a feeling for the functions F_S to F_M, we calculate a scalar box diagram with dressed vertices and propagators but keeping only the s waves in the crossed channel. Setting k = p-p', r = (p+p')/2, this is

$$\bar{F}_D(p,p') = -\frac{g^4}{i(2\pi)^4}\int d^4q\,\Delta\left(\left(\frac{k}{2}+q\right)^2\right)\Delta\left(\left(\frac{k}{2}-q\right)^2\right)V(p,r+q)$$
$$\times\, V(p,r-q)\,V(p',r+q)\,V(p',r-q)\,\bar{r}_1^{\,2}(r,q) \tag{A5}$$

where $\bar{r}_1(r,q)$ is the S-wave projection (in the $\pi\pi$ CMS) of the spinor part of the nucleon propagator. This expression has been evaluated for a number of points $p^2 = p'^2$ and k^2, and the result has been interpolated by an expression of the form with an accuracy of 10 %

$$F_{D,in} = \frac{1}{M^2}V^2(p,p')\sum_{i=1,3} a_i\,\Delta(k^2+m_i^2)\Big/\left(1-(p^2+p'^2-2M^2)/M_i^2\right). \tag{A6}$$

As mentioned in sec. 4 the D term dominates the corrections to A' and to B and is thus well determined by the WI. The interpolation function $F_{D,in}$ however is too small as to restore (2.6) by a factor of 2 at small p^2 and by a factor of 4 at large p^2. We therefore increased the masses M_2 and M_3 in (A6) by 1.2 and set

$$F_D\,(p,p') = \lambda_D\,F_{D,in}. \tag{A7}$$

The final values of the parameters are listed in Table III.

i	a_i	$m_i^2(\mathrm{GeV}^2)$	$M_i^2(\mathrm{GeV}^2)$
1	1.85	0.23	0.29
2	1.02	1.95	1.31
3	0.55	77.9	8.76
λ_S	λ_V	λ_D	λ_M
1.0	2.05	2.0	1.12

Table III: Parameters for the interpolation of the crossed box

The value of $\lambda_D = 2.0$ instead of 1.0 as expected has its origin probably in the omission of derivative πN-couplings. These occur both in the single pion exchange (where they would increase B and decrease A' if estimated from simple perturbation theory, thus requiring less box contributions) as well as in the box derivative term. The main problem is whether the remaining spin terms, namely S, V and M_i are likewise enhanced. The S-term is certainly suppressed at large momenta since it is proportional to the squared mass term $r_2^2(q'^2)$ (see (A 1), where M should be replaced by $Mr_2(q'^2)$, if q' is the internal nucleon momentum). Furthermore the higher order corrections of fig. 4 give a large negative contribution to the mass term. With Feynman parametrization and an effective coupling constant (2) $g_{eff}^2 = \frac{1}{3} g^2$ one finds that they cancel the crossed box roughly for $p^2 \approx p'^2 \approx \frac{M^2}{2}$. Since such a negative interaction is overestimated in lowest order, we multiply $F_{D,in}$ by a rapidly

decreasing function matched to the slope of the correction at $p^2 = M^2$.
We use the form

$$F_S(p,p') = F_{D,in}(p,p')/(1-(p^2+p'^2-2M^2)/M^2)^2 \tag{A8}$$

i.e. λ_S is taken as 1 in (3.4). The detailed form of $F_S(p,p')$ is not relevant, as it contributes very little to all amplitudes. Since there must be some enhancement in the derivative term, we assume that the mixed term M_i is unchanged except taking into account the mass variation in the propagator. Thus we set

$$F_M(p,p') = \lambda_M F_{D,in}(p,p')\, r_2(\bar{q}^2)/r_1(\bar{q}^2) \tag{A9}$$

where $\bar{q}^2 = \frac{1}{4}(p^2+p'^2) - M^2/2$ (A10)

is taken as the average momenteum squared of the internal nucleon. λ_M is determined by the charge normalization and turns out close to 1 (see Table III). The vector amplitude finally is calculated by multiplying in (A5) the integrand by q^2, where q is the $\pi\pi$ relative momentum. We fit the result empirically by

$$F_{V,in}(p,p') = -2.3\, F_{D,in}(p,p')(2.2M^2-p^2-p^2)((p-p')^2-20m_\pi^2)/ \tag{A11}$$
$$/((p-p')^2-100\, m_\pi^2)$$

and set $F_V(p,p') = \lambda_V F_{V,in}(p,p')$. (A11)

As mentioned in sec. 3, λ_V is determined such that the contribution of V and D to the A-amplitude cancel at large p'^2.

References

1) F. Gutbrod, DESY 72/9 (unpublished)

2) F. Gutbrod and U. Weiss, Nuclear Physics B90, 52 (1975), quoted as GW.

3) M. Böhm, Nuclear Physics B91, 494 (1975)

4) J.D. Bjorken and S.D. Drell, Relativistic Quantum Fields, McGraw-Hill, Incl., New York 1965

5) H.A. Bethe and F. de Hoffmann, Mesons and Fields II, Row, Peterson and Co., Evanston (Illinois) 1955, p. 257

6) F. Gutbrod, DESY 69/33 (unpublished); J.A. Tjon and H.M. Nieland, in The Padê Approximant in Theoretical Physics, ed. by G. Baker, Jr., and J.L. Gammel, Academic, New York 1970.

7) G. Höhler, H.P. Jakob and R. Strauss, Nucl. Phys. B39 (1972), 237

8) D. Jacobs and F. Lambert, Nucl. Phys. B63, 477 (1973)

9) R.H. Barlow, Nucl. Phys. B71, 439 (1974)

10) W.F. Nutt and L. Wilets, Phys. Rev. D11, 110 (1975)

11) S. Fishman and A. Gersten, Phys. Rev. D14, 2167 (1976)

12) P. Stichel, BI-TP 78/06 (Bielefeld 1978)